

[CONTRIBUTION FROM THE GEOPHYSICAL LABORATORY, CARNEGIE INSTITUTION OF WASHINGTON]

The System $\text{NaPO}_3\text{-Na}_4\text{P}_2\text{O}_7\text{-K}_4\text{P}_2\text{O}_7\text{-KPO}_3$

BY G. W. MOREY, F. R. BOYD, JR., J. L. ENGLAND AND W. T. CHEN

RECEIVED MAY 4, 1955

This is a study of the phase equilibrium relationships in that part of the ternary system $\text{Na}_2\text{O-K}_2\text{O-P}_2\text{O}_5$ included within the limits $\text{NaPO}_3\text{-Na}_4\text{P}_2\text{O}_7\text{-K}_4\text{P}_2\text{O}_7\text{-KPO}_3$. The binary system $\text{Na}_4\text{P}_2\text{O}_7\text{-K}_4\text{P}_2\text{O}_7$ shows a complete series of solid solutions with a minimum melting point. All compositions on the join $\text{Na}_5\text{P}_3\text{O}_{10}\text{-K}_5\text{P}_3\text{O}_{10}$ melt incongruently, there probably is a compound of the composition $\text{Na}_5\text{P}_3\text{O}_{10}\cdot\text{K}_5\text{P}_3\text{O}_{10}$, and there is extensive solid solution. The fields of these solid solution series have been determined, as well as those of the compounds NaPO_3 , $3\text{NaPO}_3\cdot\text{KPO}_3$ and KPO_3 .

This is the final paper of a series from this Laboratory on the phase equilibrium relationships in alkali phosphate systems.¹ It deals with that part of the ternary system $\text{Na}_2\text{O-K}_2\text{O-P}_2\text{O}_5$ included within the limits $\text{NaPO}_3\text{-Na}_4\text{P}_2\text{O}_7\text{-K}_4\text{P}_2\text{O}_7\text{-KPO}_3$, and it was found most convenient to represent the system by means of a quadrilateral with these compounds as the corners and the argument mole fraction K_2O and P_2O_5 (Fig. 1). The various preparations were made from two or three of the ingredients NaPO_3 , $\text{Na}_4\text{P}_2\text{O}_7$, $\text{K}_4\text{P}_2\text{O}_7$ and KPO_3 as given in Table I. Each of these ingredients was prepared by dehydration and fusion of the appropriate orthophosphate. All compositions given in the text are in the form $(\text{Na}_2\text{O}, \text{K}_2\text{O}, \text{P}_2\text{O}_5)$ in which the quantities are the mole fractions.

Experimental Methods

Melting points in this system were determined either by the quenching method, often described in papers from this Laboratory,² or by the heating-curve method. The quenching method could be used with all mixtures on, and richer in P_2O_5 than, the join $\text{Na}_5\text{P}_3\text{O}_{10}\text{-K}_5\text{P}_3\text{O}_{10}$. Mixtures on and near this join, and mixtures rich in KPO_3 , require or were given quenching in mercury; mixtures in which NaPO_3 is the primary phase and mixtures near the ternary eutectic are easily obtained as glass by removal from the furnace.

Mixtures of pyrophosphates cannot be cooled to glass and required the less convenient heating-curve method. Melts in 25-ml. platinum crucibles were used with bare thermocouple wires, carefully centered, and readings taken every 30 seconds near the break on the heating curve. There was too much undercooling to permit the use of cooling curves.

Temperatures were measured with platinum-platinum 10% rhodium thermocouples used with a White potentiometer. The couples were calibrated at the melting point of zinc,³ 419.4°; NaCl ,⁴ 800.4°; and gold,³ 1062.6°. Comparisons were frequently made with a thermocouple calibrated at the National Bureau of Standards in the International Temperature Scale of 1948. This is practically identical with the Geophysical Laboratory Scale in the temperature range under consideration.

In general the crystalline phases were identified with the petrographic microscope, by the usual technique of determining the refractive indices of the crystals by immersion in oils of known refractive index. The X-ray method of crystal identification was frequently used, but near the liquidus the amount of crystalline material is usually too small for satisfactory X-ray work. Some short cuts were frequently used. KPO_3 could be readily identified by its insolubility in water; $3\text{NaPO}_3\cdot\text{KPO}_3$ dissolved more slowly than surrounding glass, leaving isolated crystals which all dissolved in a few minutes; NaPO_3 and the triphosphates vanished with the glass. Pyrophosphates could usually be distin-

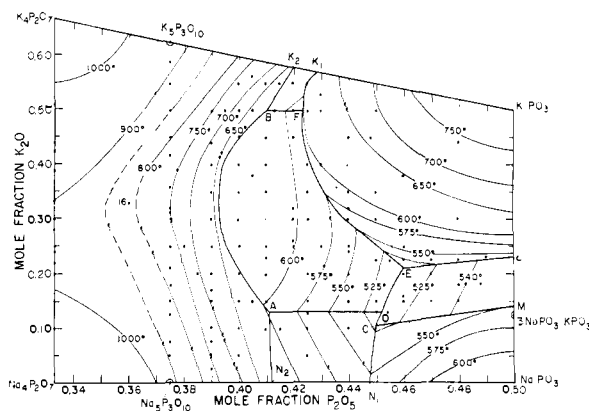


Fig. 1.—The system $\text{NaPO}_3\text{-Na}_4\text{P}_2\text{O}_7\text{-K}_4\text{P}_2\text{O}_7\text{-KPO}_3$. This diagram may be regarded as a section of the triangular diagram $\text{Na}_2\text{O-K}_2\text{O-P}_2\text{O}_5$ in which the angle at the base is changed from that of an equilateral triangle to 90°. The field of pyrophosphate solid solutions extends to the boundary N_2ABK_2 ; that of $\text{Na}_5\text{P}_3\text{O}_{10}$ is the area $\text{N}_1\text{N}_2\text{AD}$; that of $\text{Na}_5\text{P}_3\text{O}_{10}\cdot\text{K}_5\text{P}_3\text{O}_{10}$, the area ABFED ; that of $\text{K}_5\text{P}_3\text{O}_{10}$, the area FBK_2K_1 ; that of NaPO_3 , the area $\text{NaPO}_3\text{-N}_1\text{CM}$; that of $3\text{NaPO}_3\cdot\text{KPO}_3$, the area MCBL ; and that of KPO_3 , the area $\text{KPO}_3\text{-LEFK}_1$.

guished from triphosphates by their forming rounded grains resembling fish roe.

X-Ray measurements were made by the Debye-Scherrer method on a North American Phillips diffractometer with copper $\text{K}\alpha$ radiation and a nickel filter. The scanning was at 1° per minute and the recording at 2° per inch. The relative intensities are based on a scale of ten. Studies were made on both pyrophosphates and triphosphates at high temperature in a high-temperature X-ray furnace, described by MacKenzie.⁵

The Binary System $\text{Na}_4\text{P}_2\text{O}_7\text{-K}_4\text{P}_2\text{O}_7$.—Mixtures in this limiting system cannot be quenched to glass, and all melting points were determined by the method of heating curves. The melting point of $\text{Na}_4\text{P}_2\text{O}_7$ is 989°, of $\text{K}_4\text{P}_2\text{O}_7$ 1104°. The phase equilibrium results are given in no. 1-15 of Table I, and shown in the upper curve of Fig. 2. The melting point curve indicates that the two end members form a complete series of solid solutions with a minimum melting point, corresponding to Roozeboom's Type III.⁶

Under the microscope, preparations in this series characteristically show an excellent cleavage and polysynthetic twinning, which frequently assumes a crosshatched pattern. Measurements of the α and γ indices for a number of compositions are shown in Fig. 3. The 2V of intermediate compositions was checked by interference figures in

(1) E. Ingerson and G. W. Morey, *Am. Min.*, **28**, 448 (1943); G. W. Morey and E. Ingerson, *Am. J. Sci.*, **242**, 1 (1944); G. W. Morey, *This Journal*, **74**, 5783 (1952); **75**, 5794 (1953); **76**, 4724 (1954).

(2) E. S. Shepherd and G. A. Rankin, *Am. J. Sci.*, **28**, 308 (1909); G. W. Morey, "The Properties of Glass," Second Edition, Reinhold Publ. Corp., New York, N. Y., 1954, p. 32.

(3) L. H. Adams, *This Journal*, **36**, 65 (1914).

(4) H. S. Roberts, *Phys. Rev.*, **23**, 386 (1929).

(5) W. S. MacKenzie, *Am. J. Sci.*, Bowen Vol., 319 (1952).

(6) H. W. B. Roozeboom, *Z. physik. Chem.*, **30**, 385 (1899).

TABLE I
 COMPOSITION AND LIQUIDUS DATA

No.	NaPO ₃	Wt. fraction		K ₄ P ₂ O ₇	Na ₂ O	Mole fraction		Liquidus, °C.	Primary phase ^a
		Na ₄ P ₂ O ₇	KPO ₃			K ₂ O	P ₂ O ₅		
1		0.8202		0.1798	0.567	0.10	0.333	930	Pyro s.s.
2		.7350		.2650	.562	.15	.333	906	Pyro s.s.
3		.6526		.3474	.467	.20	.333	898	Pyro s.s.
4		.6205		.3795	.447	.22	.333	891	Pyro s.s.
5		.6168		.3832	.445	.222	.333	890	Pyro s.s.
6		.5887		.4113	.427	.24	.333	890	Pyro s.s.
7		.5730		.4270	.417	.25	.333	894	Pyro s.s.
8		.5574		.4426	.387	.28	.333	889	Pyro s.s.
9		.4957		.5040	.367	.30	.333	894	Pyro s.s.
10		.4461		.5539	.334	.333	.333	900	Pyro s.s.
11		.3635		.6365	.277	.39	.333	920	Pyro s.s.
12		.3140		.6860	.242	.475	.333	937	Pyro s.s.
13		.2932		.7068	.227	.44	.333	951	Pyro s.s.
14		.2900		.7100	.225	.442	.333	956	Pyro s.s.
15		.2983		.8017	.157	.51	.333	989	Pyro s.s.
16		.4064	0.1867	.4009	.31	.33	.36	825	Pyro s.s.
17	0.2724	.6394		.0852	.575	.05	.375	850	Pyro s.s.
18	.5990	.2698		.1312	.55	.075	.375	835	Pyro s.s.
19		.6925	.3075		.50	.125	.375	811	Pyro s.s.
20	.2635	.4806		.2559	.475	.15	.375	796	Pyro s.s.
21	.2600	.4353		.3047	.445	.18	.375	785	Pyro s.s.
22	.2582	.3905		.3513	.415	.21	.375	774	Pyro s.s.
23		.4985	.2987	.2068	.375	.25	.375	770	Pyro s.s.
24	.2505	.2620		.4875	.325	.30	.375	748	Pyro s.s.
25		.4073	.2882	.3045	.3125	.3125	.375	750	Pyro s.s.
26	.2490	.2316		.5194	.305	.32	.375	750	Pyro s.s.
27		.3403	.3751	.2846	.265	.36	.375	755	Pyro s.s.
28		.2633	.2847	.4520	.208	.417	.375	779	Pyro s.s.
29		.2187	.2767	.5046	.175	.45	.375	802	Pyro s.s.
30	.2360			.7640	.125	.50	.375	850	Pyro s.s.
31		.0910	.2685	.6405	.075	.55	.375	895	Pyro s.s.
32		.0541	.2664	.6795	.045	.58	.375	925	Pyro s.s.
33	.2887	.3770		.3343	.42	.20	.38	737	Pyro s.s.
34	.2841	.3051		.4108	.37	.25	.38	750	Pyro s.s.
35	.3186	.3485		.3329	.415	.20	.385	702	Pyro s.s.
36	.3686	.5875		.0439	.585	.025	.39	752	Pyro s.s.
37	.3657	.5478		.0865	.560	.050	.39	747	Pyro s.s.
38	.3627	.5081		.1295	.535	.075	.39	728	Pyro s.s.
39	.3597	.4690		.1713	.510	.100	.39	720	Pyro s.s.
40	.2539	.3932		.2529	.460	.150	.39	702	Pyro s.s.
41		.593		.407	.44	.17	.39	692	Pyro s.s.
42	.3478	.3206		.3316	.41	.20	.39	678	Pyro s.s.
								632	Pyro s.s. + NK
43	.3424	.2497		.4079	.36	.25	.39	665	Pyro s.s.
44	.3393	.2155		.4452	.335	.275	.39	660	Pyro s.s.
45		.4009	.3901	.2090	.31	.30	.39	660	Pyro s.s.
								638	Pyro s.s. + NK
46	.3318	.1148		.5534	.26	.35	.39	667	Pyro s.s.
								642	Pyro s.s. + NK
47	.3270	.0502		.6628	.21	.40	.39	675	Pyro s.s.
								642	Pyro s.s. + NK
48	.3229			.6771	.17	.44	.39	699	Pyro s.s.
49		.1339	.3673	.4988	.11	.50	.39	750	Pyro s.s.
50		.5384	.4366	.0250	.405	.20	.395	652	Pyro s.s.
								616	Pyro s.s. + NK
51		.3929	.4230	.1841	.305	.30	.395	635	NK
52		.2562	.4092	.3346	.205	.40	.395	637	Pyro s.s.
53	.3523			.6477	.185	.42	.395	682	Pyro s.s.
54		.1273	.3982	.4745	.105	.50	.395	717	Pyro s.s.
55	.4266	.4869		.0865	.55	.05	.40	681	Pyro s.s.
56	.4192	.4108		.1700	.50	.10	.40	657	Pyro s.s.
57	.4125	.3367		.2508	.45	.15	.40	643	Pyro s.s.

TABLE I (Continued)

No.	NaPO_3	Wt. fraction		$\text{K}_4\text{P}_2\text{O}_7$	Mole fraction		P_2O_5	Liquidus, °C.	Primary phase ^a
		$\text{Na}_4\text{P}_2\text{O}_7$	KPO_3		Na_2O	K_2O			
58		.5296	.4704		.40	.20	.40	627	Pyro s.s.
								617	Pyro s.s. + NK
59	.3996	.1957		.4047	.35	.25	.40	630	Pyro s.s.
60	.3932	.1286		.4782	.30	.30	.40	636	NK
61	.3876	.0632		.5492	.25	.35	.40	636	NK
62	.3818			.6182	.20	.40	.40	632	NK
63		.1839	.4350	.3811	.15	.45	.40	630	Pyro s.s.
64		.1208	.4290	.4502	.10	.50	.40	675	Pyro s.s.
65		.0594	.4231	.5175	.05	.55	.40	723	Pyro s.s.
66	.1319	.5109	.3572		.445	.15	.405	620	Pyro s.s.
								597	Pyro s.s. + NK
67		.1144	.4594	.4262	.095	.50	.405	646	Pyro s.s.
68	.4111			.5889	.215	.38	.405	625	NK
69	.4907	.4662		.0431	.565	.025	.41	629	Pyro s.s.
70	.4786	.3528		.1686	.49	.10	.41	613	Pyro s.s.
								599	Pyro s.s. + $\text{Na}_5\text{P}_3\text{O}_{10}$
71	.4711	.2800		.2489	.44	.15	.41	595	NK
72	.4629	.2107		.3264	.39	.20	.41	605	NK
73		.4680	.5320		.36	.23	.41	605	NK
74	.4562	.1423		.4015	.34	.25	.41	608	NK
75	.4488	.0767		.4745	.29	.30	.41	616	NK
76	.4423	.0125		.5452	.24	.35	.41	617	NK
77		.2341	.5119	.2540	.19	.40	.41	613	NK
78		.1700	.5047	.3253	.14	.45	.41	612	NK
79		.1077	.4973	.3950	.09	.50	.41	610	NK
80		.0473	.4817	.4710	.04	.55	.41	661	Pyro s.s.
81	.2993	.4607	.2400		.485	.10	.415	592	$\text{Na}_5\text{P}_3\text{O}_{10}$
82		.0412	.5112	.4476	.035	.55	.415	626	Pyro s.s.
83	.0194	.4107	.5699		.33	.25	.42	603	NK
84		.4095	.5905		.32	.26	.42	599	NK
85		.3541	.5825	.0634	.30	.30	.42	605	NK
86	.5008			.4992	.26	.32	.42	604	NK
87	.1571		.5576	.2853	.13	.45	.42	594	NK
88		.0953	.5478	.3552	.08	.50	.42	594	NK
89	.5746	.3408		.0846	.525	.05	.425	583	$\text{Na}_5\text{P}_3\text{O}_{10}$
90	.3600	.4020	.2380		.475	.10	.425	574	$\text{Na}_5\text{P}_3\text{O}_{10}$
91	.3017	.2986	.2997		.448	.127	.425	570	$\text{Na}_5\text{P}_3\text{O}_{10}$
92	.2531	.3955	.3514		.425	.15	.425	568	NK
93	.1492	.3896	.4612		.375	.20	.425	581	NK
94	.0487	.3837	.5676		.325	.25	.425	587	NK
95	.5308			.4692	.275	.30	.425	593	NK
96		.2790	.6053	.1157	.225	.35	.425	594	NK
97		.2138	.5964	.1898	.175	.40	.425	594	NK
98		.1505	.5877	.2618	.125	.45	.425	598	KPO_3
99		.5793	.0890	.3317	.075	.50	.425	591	KPO_3
100		.0292	.5709	.3999	.025	.55	.425	610	KPO_3
101		.3522	.6478		.28	.29	.43	584	NK
102		.2717	.6360	.0923	.22	.35	.43	585	NK
103		.2069	.6270	.1661	.17	.40	.43	596	KPO_3
104		.0828	.6087	.3085	.07	.50	.43	615	KPO_3
105		.0833	.5270	.3897	.04	.53	.43	628	KPO_3
106		.3337	.6663		.2667	.30	.4333	579	NK
107	.0094	.3249	.6657		.265	.30	.435	577	NK
108		.3244	.6756		.26	.305	.435	576	NK
109		.315	.685		.2533	.31	.4367	577	NK
110	.5570	.3234	.1196		.51	.05	.44	555	NK
111	.4468	.3180	.2352		.46	.10	.44	539	NK
112	.3398	.3128	.3474		.41	.15	.44	534	NK
113	.2363	.3080	.4557		.36	.20	.44	552	NK
114	.6222			.3778	.32	.24	.44	554	NK
115	.1353	.3036	.5611		.31	.25	.44	567	NK
116	.0388	.2980		.6632	.26	.30	.44	563	KPO_3
117		.297	.703		.24	.32	.44	578	KPO_3

TABLE I (Continued)

No.	NaPO ₃	Wt. fraction		K ₄ P ₂ O ₇	Na ₂ O	Mole fraction		Liquidus, °C.	Primary phase ^a
		Na ₄ P ₂ O ₇	KPO ₃			K ₂ O	P ₂ O ₅		
118		.2575	.6966	.0459	.21	.35	.44	596	KPO ₃
119		.1933	.6865	.1202	.16	.40	.44	622	KPO ₃
120	.643			.357	.33	.227	.443	533	NK
121	.5037	.2630	.2333		.45	.10	.45	517	NaPO ₃
122	.3398	.2598	.3004		.42	.13	.45	518	NK
123	.3965	.2589	.3446		.40	.15	.45	518	NK
124	.6836			.3164	.35	.20	.45	531	NK
125	.2417	.2532	.5051		.325	.225	.45	528	NK
126	.1925	.2507	.5568		.30	.25	.45	542	NK
127	.0950	.2469	.6581		.25	.30	.45	581	KPO ₃
128		.2433	.7567		.20	.35	.45	620	KPO ₃
129		.1182	.7345	.1473	.10	.45	.45	682	KPO ₃
130		.0583	.7244	.2173	.05	.50	.45	703	KPO ₃
131	.4614	.2391	.2995		.416	.130	.454	515	NK
132	.2455	.2466	.5079		.32	.225	.455	527	NK
133	.7146			.2854	.365	.18	.455	514	3:1
134	.2199	.2253	.5548		.295	.25	.455	557	KPO ₃
135	.5599	.2086	.2315		.44	.10	.46	533	NaPO ₃
136	.4525	.2057	.3418		.39	.15	.46	516	3:1
137	.7457			.2543	.38	.16	.46	511	3:1
138	.3489	.2022	.4480		.34	.20	.46	513	3:1
139	.3018	.1966	.5016		.315	.225	.46	533	KPO ₃
140	.2478	.1994	.5528		.29	.25	.46	562	KPO ₃
141	.1506	.1960	.6534		.24	.30	.46	596	KPO ₃
142		.1916	.8084		.16	.38	.46	665	KPO ₃
143	.7192	.1865	.0943		.495	.04	.465	568	NaPO ₃
144	.8085			.1915	.41	.12	.47	532	3:1
145	.5078	.1529	.3393		.38	.15	.47	532	3:1
146	.4040	.1506	.4454		.33	.20	.47	525	3:1
147	.3534	.1492	.4974		.305	.225	.47	535	KPO ₃
148	.8716			.1284	.44	.06	.48	573	NaPO ₃
149	.5619	.1013	.3368		.37	.15	.48	540	3:1
150	.5000	.1000	.4000		.34	.18	.48	537	3:1
151	.4067	.0995	.4938		.295	.225	.48	536	3:1
152	.2594	.0968	.6438		.20	.30	.48	620	KPO ₃
153		.0929	.9071		.08	.44	.48	739	KPO ₃
154	.9003			.0997	.4535	.062	.4845	588	NaPO ₃
155	.7453	.0613	.1934		.427	.085	.488	585	NaPO ₃
156	.54	.06	.40		.331	.181	.488	544	3:1
157	.45	.05	.50		.28	.23	.49	545	KPO ₃

^a Pyro s.s. indicates one of the series of solid solutions between Na₄P₂O₇ and K₄P₂O₇; NK indicates the compound Na₃-P₃O₁₀·K₅P₃O₁₀, 3:1 indicates the compound 3NaPO₃·KPO₃.

the course of the measurement of refractive indices by the immersion method, and some measurements of 2V were made with the universal stage. The 2V in intermediate compositions showed a range of from 0 to 25°. This much range can be found in any individual sample, and attempts to change the 2V or twinning pattern by different heat treatments were unsuccessful. The big change in 2V at the K₄P₂O₇-rich end of the system takes place closer to K₄P₂O₇ than (K₄P₂O₇)₉₄(Na₄P₂O₇)₆.

Although all compositions in the alkali pyrophosphate series appear to be one phase when examined under the microscope, it would be very difficult to interpret the refractive index plot shown in Fig. 3 on the assumption of a homogeneous solid solution unbroken by inversions. Attempts to clarify the problem by X-ray study at room temperature were abandoned, primarily because of the highly hygroscopic nature of the potassium-rich preparations. It was also found that, while small changes in the X-ray patterns of these pyro-

phosphates could be produced by different thermal treatments, these changes were not always reproducible. Accordingly, a high-temperature X-ray study of the system was undertaken with the aid of the heating stage referred to above.

A series of compositions across the system were X-rayed at a temperature of 800°, 80° below the minimum on the liquidus. The X-ray patterns so obtained showed a progressive change from Na₄-P₂O₇ to K₄P₂O₇. The amount of this shift for nine compositions was determined with quartz as an internal standard. For each composition the 2θ of the line referred to in Fig. 4 as "A" was measured relative to the quartz 101 reflection. The values so obtained, converted to d spacings and corrected for the thermal expansion of the quartz, are presented in Fig. 5. The plot shows no deviation from Vegard's law and proves that a complete solid solution exists between Na₄P₂O₇ and K₄P₂O₇ in the vicinity of the liquidus. This solid solution does not, in this temperature range, appear to be

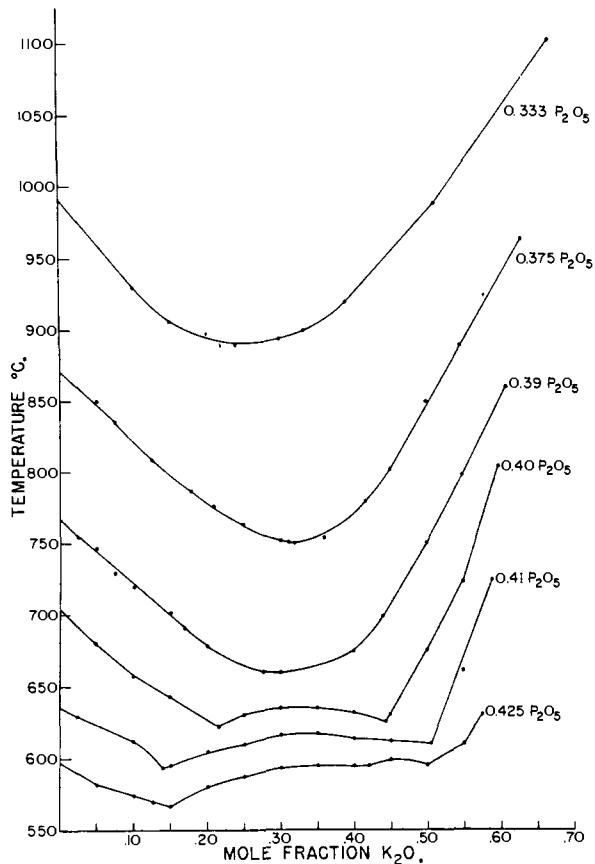


Fig. 2.—Liquidus temperatures for several series of mixtures of constant mole fraction P_2O_5 .

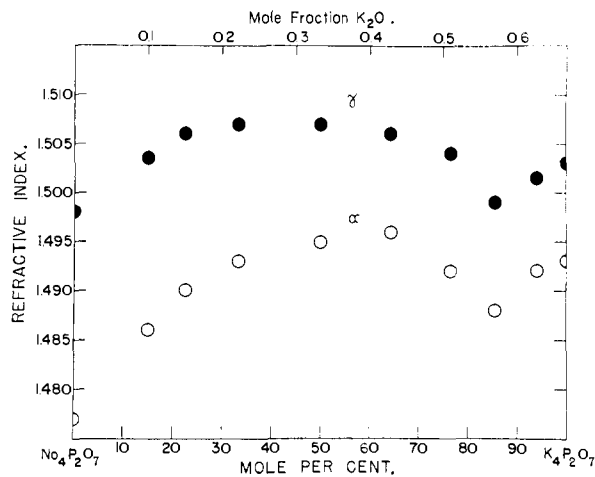


Fig. 3.—Refractive indices, α and γ , of mixtures in the binary system $\text{Na}_4\text{P}_2\text{O}_7\text{-K}_4\text{P}_2\text{O}_7$.

complicated by polymorphic inversions. Attempts to index the patterns for $\text{Na}_4\text{P}_2\text{O}_7$ and $\text{K}_4\text{P}_2\text{O}_7$ taken at 800° and to identify the reflection used in Fig. 5 were not successful.

The heating stage has also been used to investigate polymorphic transitions in the end members of this system. The technique employed was first to run series of full patterns at different temperatures for both end members. A group of these patterns is reproduced in Fig. 4. These patterns

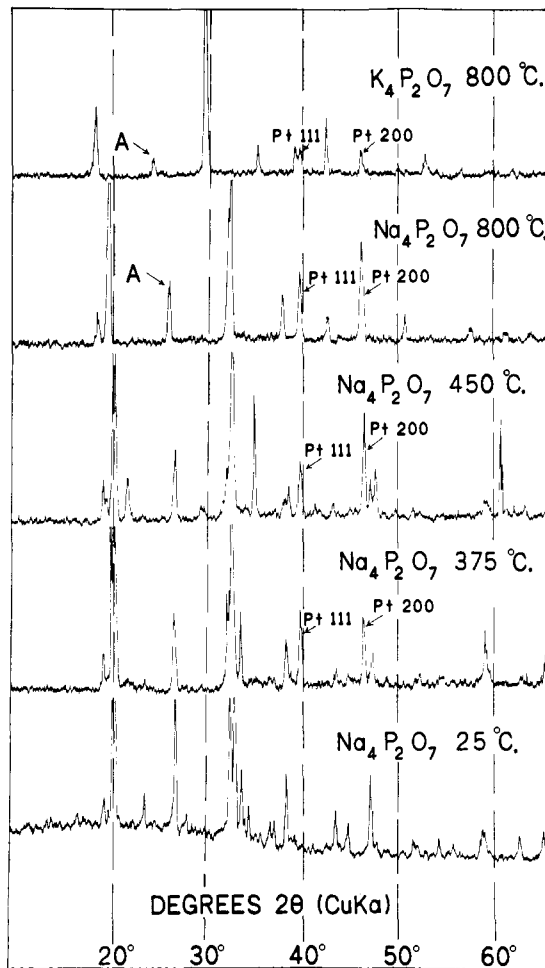


Fig. 4.—X-Ray patterns of pyrophosphates at several temperatures.

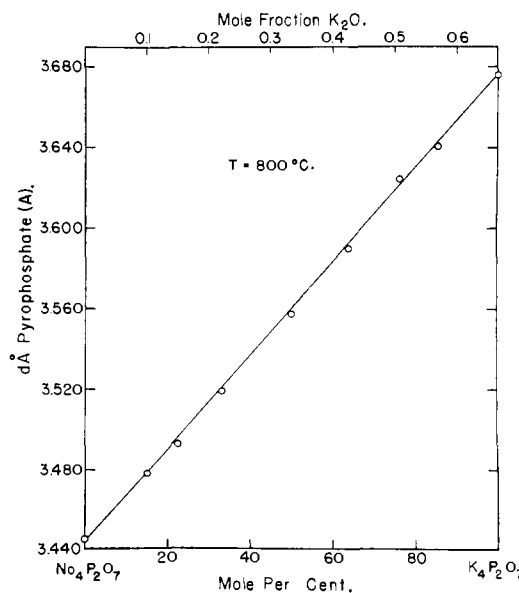


Fig. 5.—Change in 2θ with composition of solid solutions in the system $\text{Na}_4\text{P}_2\text{O}_7\text{-K}_4\text{P}_2\text{O}_7$.

sufficed to show up the different polymorphs and to rough out their temperature stability regions.

The spectrometer goniometer arm was then allowed to oscillate across a line which the previous investigation had shown to be present in one polymorphic form and not in an adjacent form. The stage was set to heat or cool across the inversion interval, and the temperature of appearance or disappearance of the key line was noted. Two polymorphic transitions in $\text{Na}_4\text{P}_2\text{O}_7$ were located in this manner. The inversion temperatures obtained are $410 \pm 10^\circ$ and $520 \pm 10^\circ$. These transitions are relatively rapid and reversible. Inversion temperatures obtained by cooling across the inversion intervals were, within the error of measurement, the same as those obtained by heating. The inversion temperatures so obtained are in agreement with the data obtained by Partridge, Hicks and Smith,⁷ although the multiplicity of inversions in $\text{Na}_4\text{P}_2\text{O}_7$ in the vicinity of 520° found by these authors was not observed in the present study.

High-temperature X-ray patterns of $\text{K}_4\text{P}_2\text{O}_7$ show only very slight changes between 350° and the liquidus. An attempt to explore these changes by the methods used with $\text{Na}_4\text{P}_2\text{O}_7$ did not yield conclusive results. An attempt was also made to locate the position of the solidus curve for $\text{Na}_4\text{P}_2\text{O}_7$ - $\text{K}_4\text{P}_2\text{O}_7$ through use of the heating camera. The technique used was similar to that employed in the investigation of polymorphic transitions. The results, however, showed too great a scatter to be useful. The scatter was due largely to crystal-melt fractionation on the tilted heating stage.

Melt no. 16 (0.31, 0.33, 0.36) between the pyrophosphates and the tripolyphosphate compositions was made in the hope that it could be quenched, since it is near the low portion of the concave liquidus surface of the pyrophosphate solid solutions. However, even the tiniest quenches invariably crystallized. From the amount of sintering of the charge, it was inferred that the liquidus is $825 \pm 10^\circ$.

The Join $\text{Na}_5\text{P}_3\text{O}_{10}$ - $\text{K}_5\text{P}_3\text{O}_{10}$.—The second section shown in Fig. 2 is the join $\text{Na}_5\text{P}_3\text{O}_{10}$ - $\text{K}_5\text{P}_3\text{O}_{10}$, which has a constant P_2O_5 mole fraction of 0.375. The liquidus results are in Table I, no. 17-32. The primary phase in all mixtures of $\text{Na}_5\text{P}_3\text{O}_{10}$ and $\text{K}_5\text{P}_3\text{O}_{10}$ is a pyrophosphate solid solution; the solidus surface coordinated with the liquidus surface was not determined. Quenches wholly free from crystals, as observed under the petrographic microscope, can be obtained only by rapid quenching in mercury.

It was difficult to prove whether or not a compound is formed along the tripolyphosphate join $\text{Na}_5\text{P}_3\text{O}_{10}$ - $\text{K}_5\text{P}_3\text{O}_{10}$. In the usual case this can be established by the shape of the melting point curve, but that is not possible here because of the incongruent melting of the tripolyphosphates. The shape of the melting point curves along the lines of constant P_2O_5 content, 0.40, 0.41 and 0.425, of Fig. 2, make it probable that there is a compound intermediate between the two end members, and a similar conclusion is indicated by the shape of the boundary curves between the pyrophosphate

and the tripolyphosphate fields in Fig. 9. In all of these the composition is far removed from the tripolyphosphate join, and the broad flat maximum on the middle portion of these curves is indicative of a strongly dissociating compound of the probable composition $\text{Na}_5\text{P}_3\text{O}_{10}$ · $\text{K}_5\text{P}_3\text{O}_{10}$. X-Ray patterns were made of a series of compositions along this join, which had been heat-treated at 500 - 550° for from 4 to 6 weeks. These patterns are assembled in Fig. 6. They indicate extensive solid solution, which may be of Roozeboom's Type II.

$\text{Na}_5\text{P}_3\text{O}_{10}$ has two crystalline modifications, but the conditions for their formation are not clear. The low-temperature⁷ form, II, is obtained when a melt is cooled slowly to about 550° and removed from the furnace, after which the melt frequently spontaneously disintegrates, as it approaches room temperature, into a powder of $\text{Na}_5\text{P}_3\text{O}_{10}$ (II). This form can be prepared by heating $\text{Na}_5\text{P}_3\text{O}_{10}$ · $6\text{H}_2\text{O}$ at 350° , but the product is not as well crystallized as that obtained by spontaneous inversion. Attempts to fix a transition temperature $\text{I} \rightleftharpoons \text{II}$ failed. When form II was heated with water in a pressure vessel at temperatures up to 400° and 750 p.s.i. pyrophosphate was formed. The transition $\text{II} \rightarrow \text{I}$ takes place quickly at 535° , slowly at 500° , in one week at 438° and not in 5 weeks at 380° . In these experiments the two forms were placed side by side, but in no case did form I change to II. We have not been able to change I to II by any treatment except the spontaneous change on cooling described above.

Sections of Constant P_2O_5 Content.—The next sections shown in Fig. 2 are those with a constant P_2O_5 content of 0.39, 0.40, 0.41, 0.425 mole fraction. All mixtures containing 0.39 P_2O_5 have a pyrophosphate solid solution as primary solid phase, and the minimum liquidus temperature, 660° , is well above the boundary between the fields of pyrophosphate solid solution and the tripolyphosphates. The section containing 0.40 P_2O_5 , however, cuts the surface of tripolyphosphate. At each end of the section pyrophosphate is the primary phase, but the central part, from about 0.25 to 0.40 K_2O , cuts the melting surface of $\text{Na}_5\text{P}_3\text{O}_{10}$ · $\text{K}_5\text{P}_3\text{O}_{10}$. The same is true of the section with 0.41 P_2O_5 . The section with 0.425 P_2O_5 cuts first the surface of $\text{Na}_5\text{P}_3\text{O}_{10}$, then the surface of $\text{Na}_5\text{P}_3\text{O}_{10}$ · $\text{K}_5\text{P}_3\text{O}_{10}$, then of KPO_3 , then of $\text{K}_5\text{P}_3\text{O}_{10}$. Sections of greater P_2O_5 content are not included in the figure because of the confusion they would cause owing to the increase in temperature from the binary eutectics to the melting points of KPO_3 or NaPO_3 .

Sections of Constant K_2O Content.—Sections through the diagram at constant K_2O content were depended on for working out the positions of the isotherms and field boundaries. The curve for mole fraction $\text{K}_2\text{O} = 0.30$ is given in Fig. 7. The melting point curve in the pyrophosphate field is steep, and the intersection with the tripolyphosphate curve at (0.307, 0.30, 0.393) and 637° is easily fixed. The crystalline phase in melt no. 45 (0.31, 0.30, 0.39) at its liquidus (660°) is a pyrophosphate solid solution. At 639° and at 633° the crystalline

(7) E. P. Partridge, V. Hicks and G. W. Smith, *THIS JOURNAL*, **63**, 454 (1941).

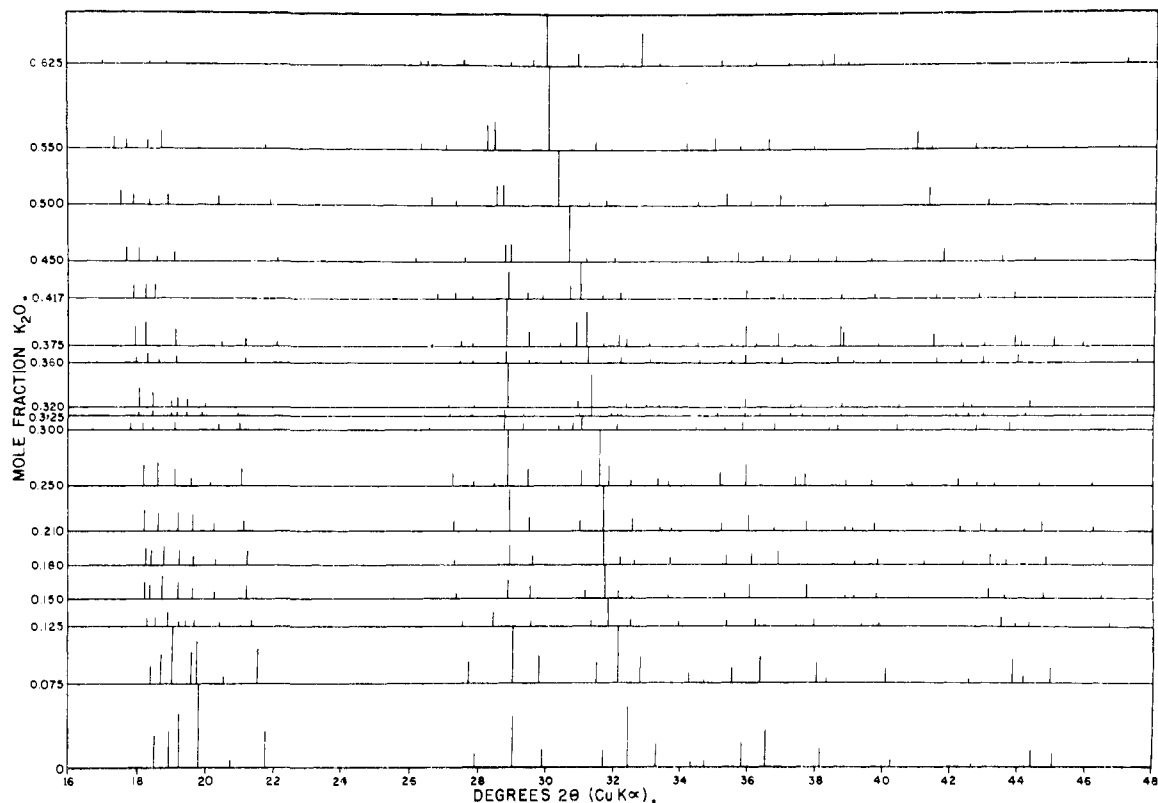


Fig. 6.—X-Ray patterns of some triphosphates.

phase is $\text{Na}_5\text{P}_3\text{O}_{10}\cdot\text{K}_5\text{P}_3\text{O}_{10}$ and gives the same X-ray patterns as no. 24 (0.325, 0.30, 0.375) at 550° and are below the metastable prolongation of the surface of the pyrophosphate solid solutions. Melt no. 51 (0.305, 0.30, 0.395) has $\text{Na}_5\text{P}_3\text{O}_{10}\cdot\text{K}_5\text{P}_3\text{O}_{10}$ as primary phase, liquidus 635° , and the intersection of the pyrophosphate and triphosphate curves fixes the boundary between the fields as (0.307, 0.30, 0.393) and 637° . The curve then falls to its intersection with the field of KPO_3 , at (0.261, 0.30, 0.439) and 568° , then rises to the

melting point of the mixture on the side $\text{NaPO}_3\text{-KPO}_3$ containing 0.30 mole fraction K_2O .

Similar curves for the mixtures containing 0.20 mole fraction K_2O are given in Fig. 8. The intersection of the pyrophosphate and the triphosphate curves is between no. 58 (0.40, 0.20, 40), liquidus 627° , and no. 124 (35, 0.20, 45), liquidus 531° . The curve for $\text{Na}_5\text{P}_3\text{O}_{10}\cdot\text{K}_5\text{P}_3\text{O}_{10}$ falls to its intersection with the field of $3\text{NaPO}_3\cdot\text{KPO}_3$, at (0.341, 0.20, 0.459) and 513° , close to the low

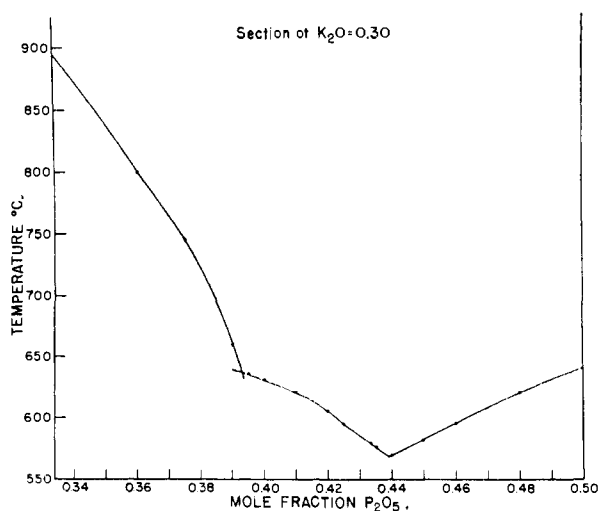


Fig. 7.—Melting points of mixtures containing 0.30 mole fraction K_2O .

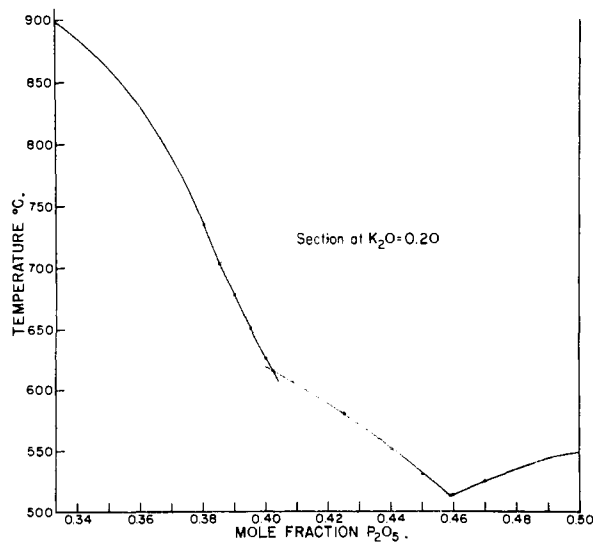
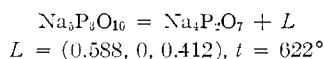


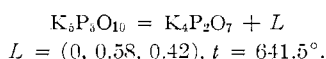
Fig. 8.—Melting points of mixtures containing 0.20 mole fraction K_2O .

eutectic at E. It then crosses the field of $3\text{NaPO}_3 \cdot \text{KPO}_3$ to the side $\text{NaPO}_3\text{-KPO}_3$. Similar curves were constructed for mixtures containing 0.10, 0.15, 0.25, 0.35, 0.40, 0.45 and 0.50 mole fractions K_2O and used for the interpolation of the isotherms of Fig. 1.

The Boundary Curves.—The boundary between the fields of the pyrophosphate solid solutions and the tripolyphosphate compounds (Fig. 9) joins the compositions of the liquids at the binary reaction points



and



The points on this boundary were determined on the lines of constant K_2O content, such as that already discussed for 0.20 and 0.30 K_2O (Figs. 7 and 8). The position of this boundary is given in the composition diagram of Fig. 1, and its temperature as a function of the K_2O content is given in Fig. 9. The temperature falls rapidly on addition of K_2O to the quadruple point A

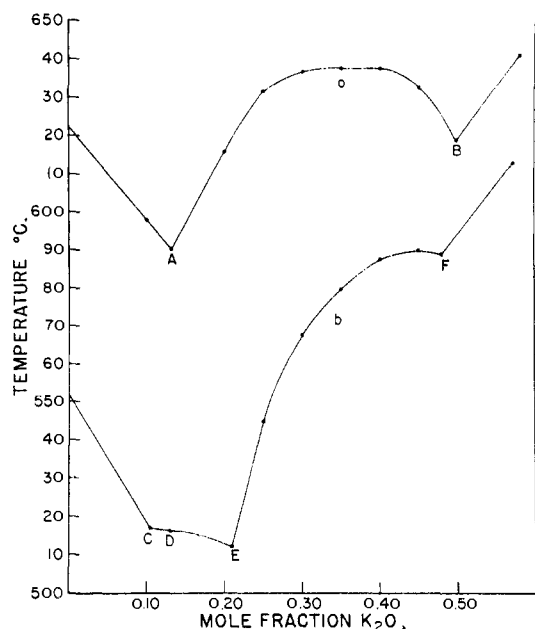
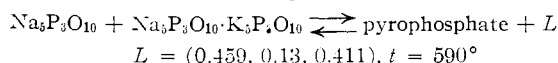
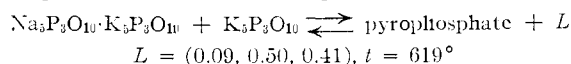


Fig. 9.—The boundary curves between the fields of pyrophosphate solid solutions and the tripolyphosphates, and between the fields of the tripolyphosphates and the three metaphosphate compounds.

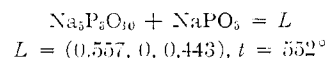
The pyrophosphate is one of the solid solution series, and each of the tripolyphosphates shows solid solution. From A, the boundary temperature increases, and the tripolyphosphate field boundary in Fig. 1 is curved to lower P_2O_5 contents, reaching its minimum P_2O_5 content at about the 1:1 $\text{Na}_2\text{O}:\text{K}_2\text{O}$ ratio. The maximum temperature on the boundary in Fig. 9 is in about the same region, but this maximum is broad and flat. The boundary

curve then goes to a higher P_2O_5 content and lower temperature at the reaction point B

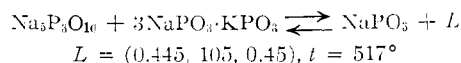


where again the crystalline phases are solid solutions. The boundary curve then rises to the binary reaction point on the side $\text{K}_4\text{P}_2\text{O}_7\text{-KPO}_3$.

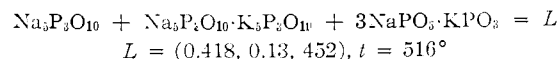
The boundary between the field of the tripolyphosphates and the fields of the three metaphosphates, NaPO_3 , $3\text{NaPO}_3 \cdot \text{KPO}_3$ and KPO_3 (Fig. 9), was located by the appropriate intersections of the several curves of constant K_2O content. The boundary starts at the eutectic in the binary system $\text{Na}_4\text{P}_2\text{O}_7\text{-NaPO}_3$, where the reaction is



then goes to the ternary reaction point C

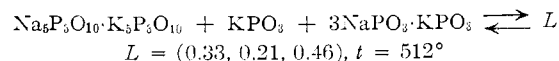


The boundary curve then goes to the invariant point D

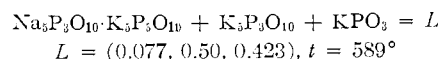


This must be a eutectic, since the composition of the liquid lies inside the triangle formed by three solid phases (Fig. 1). This triangle probably is narrow because of solid solution in the tripolyphosphate phases, and there is little discontinuity in the curve at D.

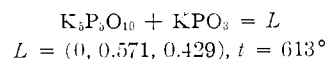
From this eutectic the boundary curve must rise slightly in temperature, then fall to the ternary eutectic E



The boundary then becomes that between the fields of $\text{Na}_5\text{P}_3\text{O}_{10} \cdot \text{K}_5\text{P}_3\text{O}_{10}$ and KPO_3 , which ends at the eutectic F



The boundary then goes to the eutectic in the binary system $\text{K}_5\text{P}_3\text{O}_{10}\text{-KPO}_3$, where the reaction is



Another curve that goes from the ternary eutectic, E, is the boundary between the fields of KPO_3 and $3\text{NaPO}_3 \cdot \text{KPO}_3$, which ends at the eutectic in the binary system $\text{NaPO}_3\text{-KPO}_3$ at 547° . Here the reaction is



and the composition of the liquid is 0.505 weight fraction KPO_3 , or (0.266, 0.234, 0.500). Similarly, the boundary between the fields of $3\text{NaPO}_3 \cdot \text{KPO}_3$ and NaPO_3 goes from the ternary reaction point, C, to the incongruent melting point of $3\text{NaPO}_3 \cdot \text{KPO}_3$ at 552° , where the reaction $3\text{NaPO}_3 \cdot \text{KPO}_3 \rightleftharpoons \text{NaPO}_3 + L$ takes place. The composition of the liquid is 0.31 weight fraction KPO_3 , or (0.36, 0.14, 0.500).

The Solid Model.—Figure 1 is the completed phase equilibrium diagram. It is a projection on

the basal plane of a prism having temperature as its vertical axis and consisting of a number of intersecting surfaces. The pyrophosphate solid solution surface is concave upward with its minimum a broad valley and sides of decreasing slope as the P_2O_5 content is increased. It intersects the tripolyphosphate surface; first the surface of the $Na_5P_3O_{10}$ solid solution series, then the surface of $Na_5P_3O_{10} \cdot K_5P_3O_{10}$, which is convex upward, as is shown by the curves of constant P_2O_5 content of 0.40, 0.41 and 0.425 P_2O_5 , of Fig. 2, then the surface of $K_5P_3O_{10}$. The change in temperature of the intersection with K_2O content is shown in Fig. 9, and the locus of compositions is indicated in Fig. 1.

The melting surface of KPO_3 sweeps down to its

intersection on the one side with the surfaces of the tripolyphosphates and on the other side with the melting surface of the compound $3NaPO_3 \cdot KPO_3$, which come together at the ternary eutectic, E. The melting surface of $3NaPO_3 \cdot KPO_3$ has a comparatively small temperature gradient, and intersects the surface for $NaPO_3$ from the incongruent melting point of $3NaPO_3 \cdot KPO_3$ on the side $NaPO_3 \cdot KPO_3$ at 552° to the reaction point C at 517° , then intersects the surface of tripolyphosphate solid solutions from the reaction point C to the eutectic, E. The surface of $NaPO_3$ intersects the surfaces of $3NaPO_3 \cdot KPO_3$ and $Na_5P_3O_{10}$, and reaches its minimum temperature at the reaction point, C.

WASHINGTON, D. C.

NOTES

Phototropic Behavior of 4-(*p*-Dimethylaminobenzeneazo)-phenylmercuric Acetate

By M. G. HOROWITZ¹ AND I. M. KLOTZ

RECEIVED MAY 18, 1955

In the course of investigations of the interaction of proteins with azomercurials, it was observed that exposure of the dye 4-(*p*-dimethylaminobenzeneazo)-phenylmercuric acetate, dissolved in certain organic solvents, to light led to a drop in the absorption of light in the region of $420 m\mu$. The absorption could be restored to its original value if the dye solution were stored in the dark. This light effect appeared to be similar to the photo-induced *trans-cis* isomerization which has been observed²⁻⁵ with other azo dyes. The isomerization reaction in the dark was studied as a function of solvent and time, since the results have a bearing on the configuration of the azomercurial in aqueous solution.

Experimental

4-(*p*-Dimethylaminobenzeneazo)-phenylmercuric acetate was prepared by a modification of the method of Jacobs and Heidelberg.⁶ The absorption spectrum of the dye was determined with a solution which had been stored in the dark overnight and also with a solution which was exposed to light before each reading. The solvents used were commercial preparations.

Optical measurements were made with the Beckman spectrophotometer, Model DU.

The rate of the *cis-trans* transformation was determined with a sample of the dye which had been dissolved in NN' -dimethylformamide (or pyridine) and exposed to illumination until the absorption at $420 m\mu$ was at the minimum value

(1) Fellow of the National Foundation for Infantile Paralysis, 1952-1954.

(2) G. S. Hartley, *Nature*, **140**, 281 (1937).

(3) G. S. Hartley, *J. Chem. Soc.*, 633 (1938).

(4) W. R. Brode, J. H. Gould and G. M. Wyman, *THIS JOURNAL*, **74**, 4641 (1952).

(5) W. R. Brode, J. H. Gould and G. M. Wyman, *ibid.*, **76**, 1856 (1953).

(6) W. A. Jacobs and M. Heidelberg, *J. Biol. Chem.*, **20**, 513 (1915).

which could be obtained with the available light intensity. The solution was then placed in the cell compartment of the spectrophotometer where it was protected from extraneous light. The increase in the optical density readings at $420 m\mu$ was recorded at intervals. The temperature at which the reaction proceeded was controlled by water circulating from a thermostated bath through the jacket surrounding the cell compartment.

If x is the optical density at $420 m\mu$ when the dye is all in the *trans*-form, y the lowest reading which can be obtained at $420 m\mu$ after exposure of the solution to light, and z the reading of the solution at $420 m\mu$ at any given time, then c_0 the initial concentration of the *cis*-dye is proportional to $(x - y)$ and c , the concentration of the *cis*-isomer at any given time, t , is proportional to $(x - z)$. Initial concentration of the *cis*-form is taken as the concentration at the moment when the solution is cut off from light.

Results and Discussion

The absorption spectrum of 4-(*p*-dimethylaminobenzeneazo)-phenylmercuric acetate dissolved in dimethylformamide is shown in Fig. 1. The spectrum of the solution maintained in the dark shows

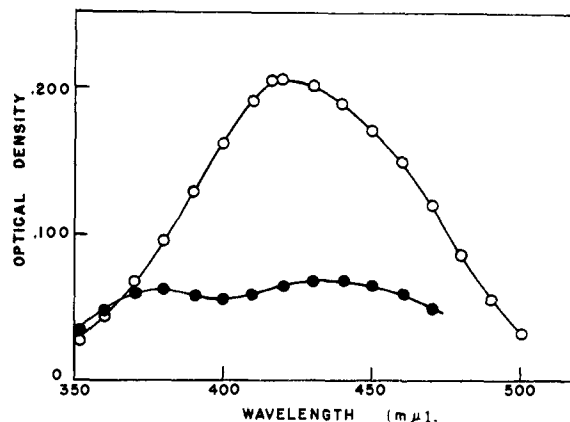


Fig. 1.—Spectrum of a $6.3 \times 10^{-6} M$ solution of 4-(*p*-dimethylaminobenzeneazo)-phenylmercuric acetate in N,N' -dimethylformamide: *trans*-form, \circ ; steady state mixture of *cis*- and *trans*-forms after exposure to light, \bullet .